Neurobiology of Aging 73 (2019) 1–10

Contents lists available at ScienceDirect

Neurobiology of Aging

journal homepage: www.elsevier.com/locate/neuaging

Intrinsic neurocognitive network connectivity differences between normal aging and mild cognitive impairment are associated with cognitive status and age

Margot D. Sullivan [a,1], John A.E. Anderson [b,1], Gary R. Turner [a], R. Nathan Spreng [c,d,e,*], for the Alzheimer's Disease Neuroimaging Initiative[2]

[a] Department of Psychology, York University, Toronto, Ontario, Canada
[b] Kimmel Family Imaging and Genetics Laboratory, Centre for Addiction and Mental Health, Toronto, Ontario, Canada
[c] Department of Neurology and Neurosurgery, Montreal Neurological Institute, McGill University, Montreal, Canada
[d] Department of Psychiatry, McGill University, Montreal, Canada
[e] Department of Psychology, McGill University, Montreal, Canada

ARTICLE INFO

Article history:
Received 16 February 2018
Received in revised form 11 September 2018
Accepted 2 October 2018
Available online 11 October 2018

Keywords:
Default mode
Dorsal attention
Frontoparietal control
Network
Mild cognitive impairment
Aging
Alzheimer's disease

ABSTRACT

Mild cognitive impairment (MCI) of the amnestic type is considered to be a transitionary stage between healthy aging and Alzheimer's disease (AD). Previous studies have demonstrated that intrinsic functional connectivity of the default network (DN) is altered in normal aging and AD and impacts both within- and between-network connectivity. Although changes within the DN have been reported in MCI, it remains uncertain how interactions with other large-scale brain networks are altered in this prodromal stage of AD. We investigated within- and between-network connectivity in healthy older adults (HOAs) and older adults with MCI across 3 canonical brain networks: DN, dorsal attention network, and frontoparietal control network. We also assessed how patterns of functional connectivity among the 3 networks predicted cognitive status and age using multivariate partial least squares. A total of 91 MCI and 71 HOA resting-state scans were analyzed from the Alzheimer's Disease Neuroimaging Initiative. There were 3 key findings. First, a circumscribed pattern of greater between-network and interhemispheric connectivity was associated with higher cognitive status in HOAs. Second, for individuals with MCI, cognitive status was positively associated with a more distributed, less-differentiated pattern of intrinsic functional connectivity across the 3 networks. Finally, greater within-network functional connectivity was positively associated with cognitive status for HOAs irrespective of age; however, this compensation-like effect diminished with increasing age for participants with MCI. Although reliable differences between healthy aging and MCI in the intrinsic network architecture of the brain are apparent, these differences emerge as shifting associations between network interactivity, cognitive functioning, and age.

Intrinsic functional connectivity within the brain, measured at rest, offers a promising avenue toward identifying early brain changes during Alzheimer's disease (AD) progression, potentially expanding the window for intervention and treatment planning (Fox and Greicius, 2010; Franzmeier et al., 2017). An important step in testing this prediction is differentiating normal from atypical network organization at the earliest disease stages. Reductions in functional connectivity between AD and healthy aging are commonly reported (e.g., see Brier et al., 2012; Damoiseaux et al., 2012; Sanz-Arigita et al., 2010; Sorg et al., 2007; Wang et al., 2007; see Damoiseaux, 2017; Dennis and Thompson, 2014; Grady, 2012; Teipel et al., 2016 for reviews). However, identifying brain differences in prodromal disease stages such as mild cognitive impairment (MCI) has proven more challenging, with myriad and often conflicting reports of both increases and decreases in network connectivity (e.g., Damoiseaux et al., 2012; Jones et al., 2016; Wang et al., 2015).

Although global changes in network connectivity have been reported in both MCI and AD (Sanz-Arigita et al., 2010), much of the research examining cortical brain differences between typical aging

* Corresponding author at: Montreal Neurological Institute, 3801 rue University, Montréal, Québec H3A 2B4, Canada. Tel.: +1 5142489775; fax: +1 5143988248.
E-mail address: nathan.spreng@gmail.com (R.N. Spreng).

[1] These authors contributed equally to the manuscript and share first authorship.

[2] Data used in preparation of this article were obtained from the Alzheimer's Disease Neuroimaging Initiative (ADNI) database (adni.loni.usc.edu). As such, the investigators within the ADNI contributed to the design and implementation of ADNI and/or provided data but did not participate in analysis or writing of this report. A complete listing of ADNI investigators can be found at http://adni.loni.usc.edu/wp-content/uploads/how_to_apply/ADNI_Acknowledgement_List.pdf.

0197-4580/$ – see front matter © 2018 Elsevier Inc. All rights reserved.
https://doi.org/10.1016/j.neurobiolaging.2018.10.001

and neurodegenerative disease has targeted the default network (DN) of the brain. The DN is an assembly of functionally connected regions, including anterior (medial prefrontal cortex) and posterior (posterior cingulate) hubs along the midline, as well as subnetworks including lateral and medial temporal lobe structures (Andrews-Hanna et al., 2014). Functionally, the DN is associated with internally directed cognitive processes, including memory functions, making this network an early focus of research to identify biomarkers of cognitive decline in MCI and AD (Damoiseaux, 2017). Longitudinal analysis of the DN suggests that within-DN functional connectivity follows an inverted U-shaped curve and these changes predict episodic memory and processing speed (but not working memory or executive functions). Early in the aging process (<66 years), functional connectivity increases before leveling off (66–74 years) and finally sharply declines (>74 years) (Staffaroni et al., 2018).

Early studies of neurodegenerative changes within the DN implicated the hippocampus and entorhinal cortex and reduced connectivity between these medial temporal lobe structures and other DN regions, including the posterior cingulate hub, in persons at risk for AD (Sorg et al., 2007). In clinical stages of the disease, these structural brain changes in medial temporal subregions project to the cortical mantle, following a spatial topology that closely overlaps the DN (Buckner, 2004; Buckner et al., 2005; Damoiseaux, 2017; Hafkemeijer et al., 2012; Khan et al., 2014; Spreng and Turner, 2013). DN hub regions also show greater susceptibility to accelerated amyloid accumulation, structural atrophy, and metabolic changes in AD (Buckner, 2004; Buckner et al., 2005), and the network may serve as a vector for transmission of AD-related neuropathies across the cortex (Buckner et al., 2008; Buckner et al., 2005; Seeley et al., 2009).

There is recent evidence that these DN changes may initiate a cascade of network failures resulting in the eventual conversion from normal aging to AD (Jones et al., 2016). This suggests that network changes within the DN provide only a partial account of altered functional connectivity changes in the disease. Within-network changes have been shown to co-occur with altered connectivity between the DN and other large-scale brain networks both in typical aging (Chan et al., 2014) and AD (Brier et al., 2012). Critically, between-network changes may not follow a linear pattern of decline but may proceed in discrete stages, first involving increased connectivity between DN and frontal association cortices, followed by declining within- and between-network connectivity later in the disease course (Damoiseaux, 2017; Jones et al., 2016). Thus, changing patterns of within- and between-DN connectivity may serve as a better marker of early brain changes in MCI and AD, and there is initial evidence for this idea (Wang et al., 2015; Zhan et al., 2016).

Three canonical large-scale networks, the DN, dorsal attention network (DAN), and the frontal parietal control network (FPCN), have been identified as stable features of the functional architecture of the brain during task and rest (Spreng et al., 2013). As with the DN, functional connectivity within the DAN and FPCN declines in typical aging (Andrews-Hanna et al., 2007; Avelar-Pereira et al., 2017; Grady et al., 2016; Li et al., 2012; Spreng et al., 2016; Tomasi and Volkow, 2012; Turner and Spreng, 2015) and changes are accelerated in AD (Brier et al., 2012; Damoiseaux et al., 2012; Franzmeier et al., 2017; Wang et al., 2015; Zhan et al., 2016). These within-network declines co-occur with changes in between-network connectivity, and this shifting network architecture may be compensatory in MCI (Wang et al., 2015; Zhan et al., 2016). Failure of this system may mark the transition to the clinical phase of the disease. Reduced intranetwork connectivity within the DN and DAN has recently been linked to increased between-network connections with the FPCN, and these changes were associated with better cognitive performance in normal aging (Grady et al., 2016). Whether this compensatory-like pattern of network dynamics is preserved or disrupted in MCI remains uncertain.

To investigate whether neural network organization is preserved or disrupted in MCI, we measured within- and between-network differences in the DN, DAN, and FPCN and use a novel approach to examine how changes in this network architecture are associated with cognition and age in normal aging and MCI cohorts from the Alzheimer's Disease Neuroimaging Initiative (ADNI) data set. There are 2 specific aims. The first is to contrast the intrinsic functional connectivity of the DN, FPCN, and DAN in healthy aging compared to MCI. The second aim is to investigate how this intrinsic architecture interacts with both cognitive status and age, and how these brain and behavioral associations may differ between normal aging and MCI. We predict reduced within-network functional connectivity for MCI as compared to normal aging for each of the networks. Extending the findings of Grady et al. (2016), we further predict that individuals with MCI will demonstrate greater between-network connectivity among the DN, DAN, and FPCN. However, the strength of this between-network coupling in MCI will be associated with lower cognitive status, signaling an emerging failure of compensation-like reorganization in this prodromal stage of AD.

1. Methods

1.1. ADNI database

Data used in the preparation of this article were obtained from the ADNI database (adni.loni.usc.edu). The ADNI was launched in 2003 as a public-private partnership, led by Principal Investigator Michael W. Weiner, MD. The primary goal of ADNI has been to test whether serial magnetic resonance imaging (MRI), positron emission tomography (PET), other biological markers, and clinical and neuropsychological assessment can be combined to measure the progression of MCI and early AD.

1.2. Study sample and search criteria

All available rs-fMRI and associated T1 structural data from the ADNIGO/ADNI2 phases with a diagnostic status of MCI or normal (healthy older adult [HOA]) were downloaded on July 18, 2015–22, 2015. Group diagnostic criteria are available publically in the ADNI procedures manual (see https://adni.loni.usc.edu/wp-content/uploads/2008/07/adni2-procedures-manual.pdf). Participants are classified as cognitively normal if there are no current memory concerns above typical age-related changes and cognition and daily living is unimpaired. HOA and MCI groups have a Mini–Mental Status Examination (MMSE, Folstein et al., 1975) score within the range of 24–30. A diagnosis of MCI includes a subjective memory concern accompanied by abnormal performance on the Logical Memory II subscale from the Wechsler Memory Scale-Revised (Wechsler, 1945) and a Clinical Dementia Rating of 0.5. MCI participants do not meet the criteria for probable AD in terms of cognitive and daily functioning. As all participants in both HOA and MCI groups had a reported MMSE score, and the measure assesses multiple domains of cognition, we selected this as our measure of cognitive status. Importantly, MMSE was not used as criteria for MCI diagnosis in the ADNI.

The earliest dated rs-fMRI scan was selected per roster ID (RID) to assess baseline functional connectivity. The initial search resulted in a total of 102 MCI and 79 HOA images. From this sample, 11 MCI and 8 HOA scans were excluded. Exclusions were based on having a quality control rating of 4 (rated by the ADNI quality control team at the Mayo clinic), unusable (1 MCI, 4 HOA), use of a different rs-fMRI protocol (1 MCI), or a repetition time < 3000 ms (6 MCI, 1 HOA). In addition, temporal signal-to-noise ratios (tSNRs)

were calculated per participant and per network region of interest (ROI) after preprocessing was complete by dividing the temporal mean image by the standard deviation. A poor tSNR was considered using a threshold <100 (Jones et al., 2016). Three MCI and 3 HOA participants had 5 or more ROIs within the DN, DAN, or FPCN (see below for ROI information) with a tSNR < 100 and were excluded (5 ROIs being 2.5 standard deviation outside of the sample mean). The final analysis sample included 91 MCI and 71 HOA images (see Supplementary Table 1 for RIDs and image IDs).

1.3. Functional MRI data acquisition and preprocessing

ADNI participants were scanned using 3T Philips MRI scanners and an 8-channel head matrix coil. rs-fMRI data were acquired with eyes open and single-shot gradient echo planar imaging (EPI), with 140 volumes (repetition time = 3000 ms, echo time = 30 ms, flip angle = 80°, 48 transverse slices, 64 × 64 matrix, and 3.3 mm of isotropic voxel resolution). Anatomical scans were acquired with a 3-dimensional (3D) MPRAGE sequence using SENSE (repetition time = 6.8 ms, echo time = 3.1 ms, 1.1 (FH) × 1.1 (AP) × 1.2 (RL) mm voxel resolution, FOV = 270 (FH) × 253 (AP), 244 × 244 acquisition matrix, reconstructed as a 256 × 256 matrix, 170 sagittal slices of 1.2-mm thickness, acceleration factor of 2). Full descriptions of ADNI MRI protocols are available at http://adni.loni.usc.edu/methods/documents/mri-protocols/.

All image preprocessing was completed using FMRIB Software Library (FSL) (www.fmrib.ox.ac.uk/fsl) (Jenkinson et al., 2012; Smith et al., 2004). First, FSL BET (Smith, 2002) was run to remove the skull and any nonbrain tissue from the structural T1 image scans. Second, FSL FEAT was used to preprocess the functional image data. This included deleting the first 4 volumes, motion correction using MCFLIRT (Jenkinson et al., 2002), interleaved slice-timing correction, spatial smoothing with an 8-mm FWHM gaussian kernel, high-pass temporal filtering with a cutoff of 100 seconds, MELODIC ICA denoising, and registration to the MNI template. Registration to high-resolution structural and standard space was performed using FLIRT (Jenkinson et al., 2002; Jenkinson and Smith, 2001) and an MNI152 standard-space T1-weighted 2-mm average structural template image. Next, FSL FIX (Griffanti et al., 2014; Salimi-Khorshidi et al., 2014) was used to automatically classify noise ICA components from the data. In the first pass, the Standard.RData training weight provided by the FIX program was used to classify the components (see https://fsl.fmrib.ox.ac.uk/fsl/fslwiki/FIX/UserGuide). After the initial running of FIX, a random subset (n = 25) of the data was manually examined to verify if the components were accurately labeled as signal or noise (e.g., motion, vascular, or non–gray matter tissue signal). FIX was then rerun on the entire sample using the newly hand-trained, classifier. In terms of motion, there were no group differences in the signal intensity metric, DVARS (Power et al., 2012, 2013), that was calculated from the initial non-preprocessed time series data ($p = 0.92$), nor were there any group differences in head displacement along the 6 motion parameter estimates generated from MCFLIRT (p's > 0.19).

1.3.1. CONN toolbox

Following preprocessing, rs-fMRI data were processed using the MATLAB-based, CONN toolbox (Whitfield-Gabrieli and Nieto-Castanon, 2012), to calculate bivariate correlation matrices for each individual scan using ROIs from the study by Spreng et al. (2013) and replicated in the study by Grady et al. (2016). Nodes were represented by spherical ROIs, with a 5-mm radius, centered on the aforementioned coordinates. Following the procedure used by Spreng et al. (2013), the overlapping voxel situated in the left hemisphere between the dorsolateral prefrontal cortex and the middle frontal gyrus (BA 9) was removed before analysis. As it has been documented that there is decreased signal in the left lateral frontal lobe of the ADNI data set (see Jones et al., 2016), we examined the tSNR for each participant's ROIs. Two ROIs had a tSNR < 100 for 33% and 28% of participants, respectively, and were approximately +2.5 standard deviation from the mean n per ROI for each group. These ROIs were the left anterior temporal lobe ($n_{MCI} = 30$, $n_{HOA} = 24$) and the left ventral medial prefrontal cortex ($n_{MCI} = 21$, $n_{HOA} = 25$). These 2 ROIs were removed, leaving 41 ROIs for analysis.

We used CONN toolbox to calculate the between-ROI, r-to-z Fisher-transformed, bivariate correlation matrices per participant based on the standardized T1 and rs-fMRI data. Sources of noise that were regressed out included 6 motion parameters (participant.par files), 5 principal components analysis temporal components from the cerebrospinal fluid and white matter masks generated, as well as motion outliers detected by ArtRepair-based motion scrubbing. ArtRepair outlier detection was set to 2 standard deviation from the z-normalized global mean signal and to 0.5 mm for the movement threshold. Linear detrending was performed, and a band-pass filter of 0.01–0.1 Hz was applied to the data following regression of confounding variables.

1.3.2. Behavioral partial least squares analyses

We used behavioral partial least squares (PLS), a multivariate technique similar to principal components analysis (see Krishnan et al., 2011; McIntosh et al., 1996, 2004, for an in-depth description of this method), to analyze the relationship between the interregional connectivity matrices, cognitive status, age, and diagnostic group. Behavioral PLS computes the maximum covariance between brain and behavioral data (MMSE, age) by performing singular value decomposition (SVD) on the stacked condition-wise matrix, (i.e., for each group, across participants, there will be 2 stacked submatrices representing the relationship between each behavioral variable and the brain data). SVD evaluates brain-behavioral patterns from the stacked data matrix in terms of orthogonal singular vectors, known as saliences. Latent variables (LVs) therefore represent the maximum covariance between linear combinations of the original brain and behavior data matrices and the computed saliences. The significance of each LV is determined through permutation testing, and reliability is determined through a bootstrap estimation of the standard errors for the brain saliences.

During permutation testing, the data matrix rows are rearranged without replacement and SVD is repeated to identify LVs. By completing this process n times, a probability value can be determined to assess how frequently the permutated singular values surpass the original values. During bootstrap testing, sampling with replacement and PLS is completed n times to determine the standard error of the brain saliences. The salience is divided by the standard error of the bootstrap, providing a bootstrap ratio (BSR). The BSR is comparable to a Z score, and BSRs ≥ 2 are considered reliable (Grady et al., 2000; Krishnan et al., 2011). Because the analysis is computed in a single analytic step, no corrections for multiple comparisons are required (McIntosh et al., 2004). Significance was tested by computing the result to a null distribution generated from 500 permutations. In addition to the BSRs, the confidence intervals (CIs) for the brain-behavior correlations were calculated using 500 bootstrap samples, to determine reliable associations. Resulting brain-network graphs were thresholded at a BSR of ±2 and were visualized using the BrainNet Viewer (Xia et al., 2013).

2. Results

2.1. MMSE and age

Independent samples t-tests were performed to compare the 2 groups on MMSE score and age in years (see Table 1 for group

Table 1
Mean (standard deviations) MMSE scores and age in years by group

Group	n	MMSE	Age
MCI	91	27.99 (1.66)	71.96 (7.76)
HOA	71	28.90 (1.27)	74.10 (6.71)

Key: HOA, healthy older adult; MCI, mild cognitive impairment; MMSE, Mini–Mental Status Examination.

means). Levene's test was used to assess for equality of variances. As Levene's test was significant for MMSE scores, $F(1, 160) = 8.90$, $p = 0.003$, the t-test statistic was calculated using unpooled variances and degrees of freedom were adjusted in SPSS using the Satterthwaite correction. There was a significant group difference for MMSE scores, $t(159.95) = -3.97$, $p < 0.001$, $d = -0.63$, such that the MCI group had lower scores than the HOA group. The comparison between groups for age did not reach statistical significance, $t(160) = -1.85$, $p = 0.07$, $d = -0.29$. To eliminate the possibility of ceiling effects, simple t-tests were run on the variable MMSE score against the value of 30 (i.e., the maximum score that can be obtained) for each group and the combined sample. This was performed to ensure that the behavioral PLS results should not be attributable to ceiling effects of MMSE scores. There was a significant difference from the value of 30 for the MCI group, $t(90) = -11.58$, $p < 0.001$, $d = -1.2$, HOA group, $t(70) = -7.31$, $p < 0.001$, $d = -0.87$, and the combined sample, $t(161) = -13.13$, $p < 0.001$, $d = -1.0$.

2.2. Network analysis

First, we examined differences in the network architecture between groups. Fig. 1 displays r-to-z Fisher-transformed correlation matrices by group. A PLS analysis using these matrices as inputs failed to generate a significant group effect, LV1, $p = 0.998$. The heat maps are similar across groups, with the mean of the difference matrix (HOA − MCI) equal to −0.01 (min = −0.13, max = 0.12) and a correlation between matrices of $r = 0.96$.

2.3. Network, age, and cognitive status analysis

Next, we assessed how the neurocognitive network architecture varies as a function of age and cognitive status. The first significant LV dissociated distinct patterns of intrinsic connectivity differences between MCI and HOA groups (LV1, $p = 0.012$, 36% covariance explained; Fig. 2). In the HOA group, MMSE and age covaried

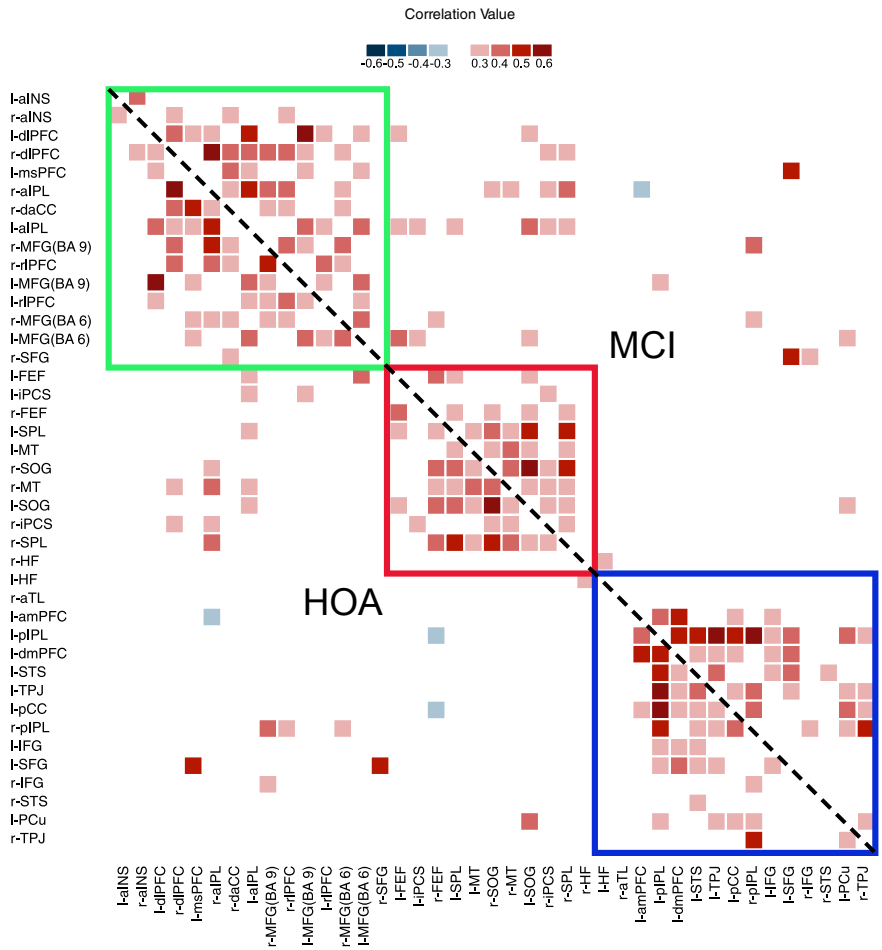

Fig. 1. Non-symmetrical correlation matrix of thresholded resting state correlations by group. Networks affiliation is indicated by color: green represents the frontoparietal control network, red represents the dorsal attention network, and blue represents the default network. Correlations for HOA fall below the diagonal, while correlations for the MCI group fall above the diagonal. aINS, anterior insula; aIPL, anterior inferior parietal lobule; amPFC, medial prefrontal cortex; aTL, anterior temporal lobe; BSR, bootstrap ratio; daCC, dorsal anterior cingulate cortex; dlPFC, dorsolateral prefrontal cortex; dmPFC, dorsal medial prefrontal cortex; FEF, frontal eye fields; HF, hippocampal formation; HOA, healthy older adults; IFG, inferior frontal gyrus; iPCS, inferior precentral sulcus; l-, left hemisphere; LV1, first significant latent variable; LV2, second significant latent variable; MCI, mild cognitive impairment; MFG (BA 6), middle frontal gyrus, BA 6; MFG (BA 9), middle frontal gyrus BA 9; MMSE, Mini–Mental Status Examination; msPFC, medial superior prefrontal cortex; MT, middle temporal motion complex; pCC, posterior cingulate cortex; PCu, precuneus; PFC, prefrontal cortex; pIPL, posterior inferior parietal lobule; r-, right hemisphere; rlPFC, rostrolateral prefrontal cortex; SFG, superior frontal gyrus; SOG, superior occipital gyrus; SPL, superior parietal lobule; STS, superior temporal sulcus; TPJ, temporal parietal junction.

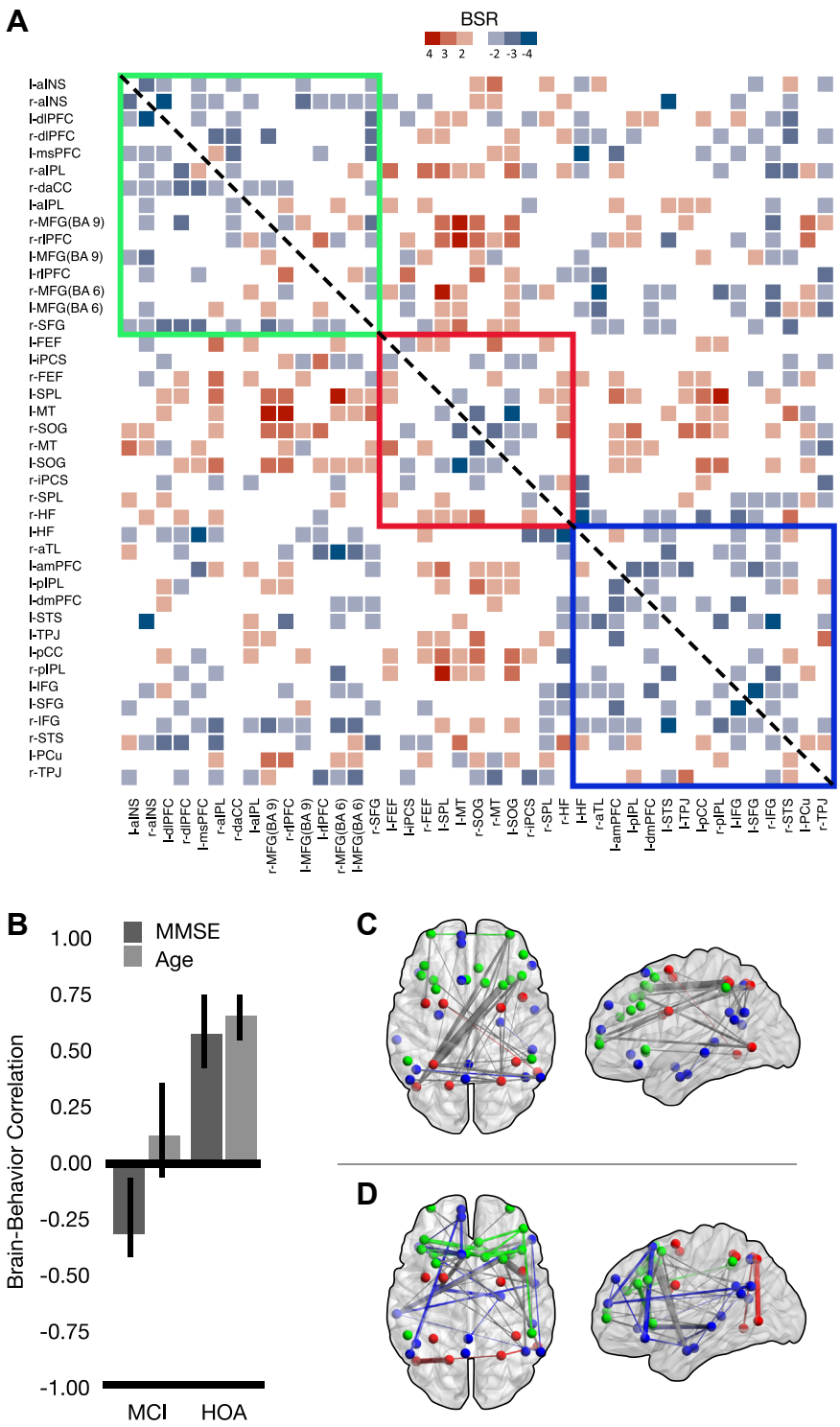

Fig. 2. Symmetrical BSR matrix of brain-behavior covariances for LV1 (panel A) displaying thresholded BSR values for MMSE and age effects. The matrix is thresholded at ±2 to 6. Panel B displays the relationship between MMSE and age with brain connectivity by group. Confidence intervals are 95% BSRs. Panel C represents the positive BSR values from the covariance matrix (A) between MMSE, age, group, and functional connectivity in brain space. Panel D represents the negative BSR values. Panels A, C, and D are color coded by network: green represents the frontoparietal control network, red represents the dorsal attention network, and blue represents the default network. For panels C and D, within-network connections are colored according to network affiliation, and between-network connections are colored gray. See Fig. 1 caption for abbreviations.

together with a selective pattern of interhemispheric and internetwork connectivity. In the MCI group, only MMSE was associated with a pattern of connectivity that showed stronger global integration of the 3 networks. Bar graphs in Fig. 2 (panel B) describe the average correlations between the graph and MMSE and age with 95% bootstrapped CIs. Reliable differences can be ascertained by lack of overlap of the 95% bootstrapped CI. The anatomically constrained functional connectivity graphs for LV1 are presented separately by positive (panel C) and negative (panel D) BSR values.

The brain-behavior correlations (panel B) indicate that within the HOA group, those individuals who (1) have higher MMSE scores and (2) are older show more internetwork and interhemispheric

connections. This pattern was particularly evident across the right FPCN and left DAN networks, and integrated nodes of the DN, represented by the positive brain-score network (panel C). MCI individuals show no relationship between the positive brain-score network and age but show a negative correlation with MMSE. The interregional connections that were *positively* correlated with MMSE scores (and age) in HOAs were associated with *lower* MMSE scores in the MCI group. Negative brain scores (panel D) were associated with a network configuration showing a globalized pattern of network degradation and dedifferentiation. For individuals with MCI, this loss of differentiated network connectivity was positively associated with higher MMSE scores suggesting a compensatory-like brain response within this group. In contrast, this pattern was associated with *worse* MMSE scores and *younger* ages in HOAs, clearly reflecting a maladaptive functional architecture for these participants.

A second significant LV emerged from this analysis (LV2, $p = 0.028$, 26% covariance explained; Fig. 3). The brain-behavior correlation pattern (panel B) shows that for both groups, those individuals who have higher MMSE scores tended to have greater DN functional connectivity, centered around a precuneus hub, and greater DN cross-network integration with the FPCN, represented by the positive brain-score network (panel C). Greater DN functional connectivity appears to benefit cognition for both groups after accounting for group-specific network patterns identified in LV1. HOA individuals show no relationship between brain-scores and age as the CI overlaps zero. MCI individuals display a negative correlation with age, such that individuals who are older show less within-network and more irregular patterns of network functional connectivity (panel D).

2.4. Within-group analyses

To decompose the multivariate interaction of age, MMSE, and group, we conducted 4 additional exploratory analyses. We first present the results of the within-group analyses (see Fig. 4). For each comparison, which again used age and MMSE as covariates of resting-state functional connectivity, only the first LV was retained, as latter LVs were not significant. The within-group analysis for HOAs was significant, $p = 0.02$, 64% covariance explained, and largely replicated the pattern seen in the first LV of the between-group analysis. The correlation between the BSR matrix of the first LV for the HOA group and the first LV of the between-group analysis was 0.98. Conversely, the BSR matrix of the first LV for the HOA group did not correlate strongly with the second LV of the grouped analysis, $r = 0.16$.

Next, we examined the pattern of functional connectivity with age and MMSE in the MCI group. The first LV approached the threshold for significance, $p = 0.06$, 60% covariance explained. The BSR matrix for the first LV representing the MCI group correlated most strongly with the *second* LV of the original between-group analysis, $r = 0.95$, and was weakly correlated with the first LV of the between-group analysis, $r = 0.21$. The above analyses now allow us to reconceptualize our understanding of the original between-group analysis. The first LV predominantly represents *healthy aging*, whereas the second LV predominantly represents abnormal aging, or *MCI*. We next analyzed the effects of age and MMSE in separate analyses, but as neither reached significance, both p values > 0.09, these findings are not considered further.

2.5. Additional memory measures

Finally, to address whether these results were potentially biased by our choice of the MMSE, which may have been considered as part of the diagnostic tools used to identify patients with MCI, we replaced MMSE scores with 2 independent measures of memory (immediate and delayed memory recall from the Logical Memory test of the Wechsler Memory Scale-Revised, Wechsler, 1945), in a subgroup of the original sample (MCI, N = 81; HOA, N = 64). Both analyses reproduce the findings of the original between-group analysis using MMSE (see Supplementary Fig. 1). This suggests that the main results did not depend on the MMSE as a cognitive measure.

3. Discussion

We investigated the integrity and interactivity of the DN, FPCN, and DAN, and associations with cognitive functioning, in healthy aging and MCI. Although the topology of each network was generally preserved across groups (see Fig. 1; Grady et al., 2016; Spreng et al., 2013), group differences began to emerge once the impact of age and cognition was considered. Specifically, greater interactivity (1) between brain networks and (2) across hemispheres was associated with better cognitive performance in HOAs. Moreover, this association was stronger with increasing age in this group, suggesting an age-related, compensatory-like pattern of network dedifferentiation (Grady et al., 2016). Critically, however, this same pattern of network dedifferentiation was associated with worse cognition in MCI, irrespective of age. This suggests that for individuals who develop MCI, there may be an inflection point, where intrinsic network dedifferentiation may no longer follow a compensatory-like pattern, resulting in the emergence of subjective and objective cognitive decline and MCI.

Higher cognitive performance has been associated with less reconfiguration of brain networks between task and rest states in younger (Schultz and Cole, 2016) and older (Grady et al., 2016) adults. This latter study observed age-related increases in network reconfiguration specifically *within* the FPCN and the DN. Although we do not include task data here, HOAs do show greater network connectivity at rest. Compared to the MCI group, HOAs maintain more connections within network (see Fig. 2) as well as engaging more between-network and cross-hemisphere connections, possibly reflecting compensatory-like processes. Given these more distinct network connectivity patterns, the HOA results here appear more similar to the younger adult patterns in these earlier studies than to the more dedifferentiated patterns observed for our MCI group. However, rest-to-task interactions remain an area of future investigation in early AD.

Our primary analysis integrated network connectivity, cognition, age, and diagnostic status within a single multivariate model. This allowed us not only to interrogate changes in brain network dynamics between groups but also to explore how these network changes differentially related to cognitive capacity in normal aging and MCI. For HOAs, age and cognitive status (MMSE) were positively associated with stronger within- and between-network connections across hemispheres (see Fig. 2, panel C). This suggests that normal cognitive aging may reflect compensatory reorganization of intrinsic functional networks involving greater network interactions. This finding is consistent with a recent report showing greater FPCN interactivity with the DAN and DN was associated with better memory performance (Grady et al., 2016). Furthermore, this compensation-based interpretation is consistent with models of neurocognitive aging suggesting that increased recruitment of anterior brain regions (Davis et al., 2008) and less-lateralized patterns of functional brain response (Cabeza, 2002) are associated with better cognitive performance. Posterior regions of the DN are among the most susceptible to neuropathological changes in AD, often showing the earliest structural and functional brain changes (Andrews-Hanna et al., 2014; Buckner, 2004; Damoiseaux, 2017). Here, the precuneus and the posterior

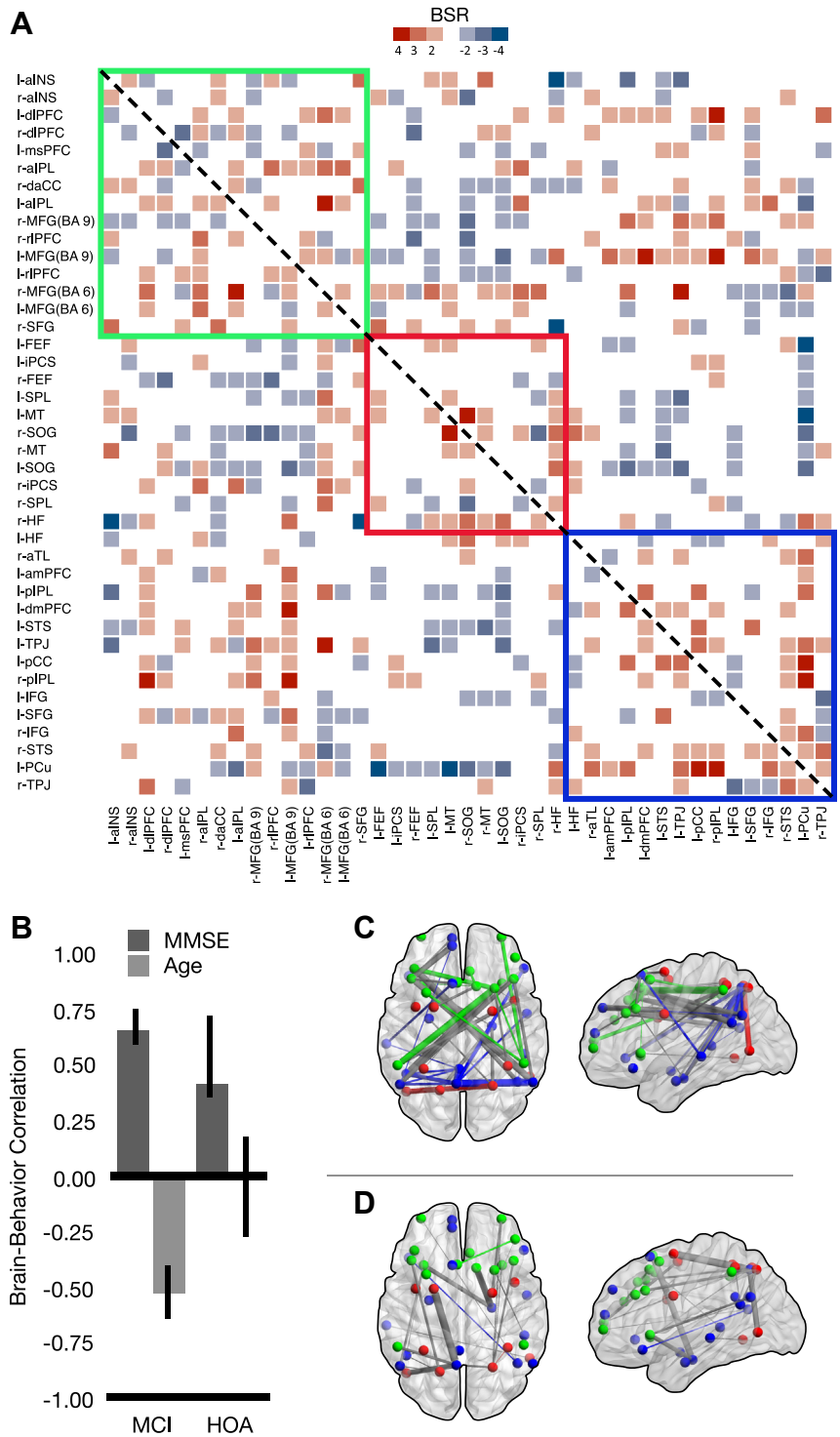

Fig. 3. Symmetrical BSR matrix of brain-behavior covariances for LV2 (panel A) displaying thresholded BSR values for MMSE and age effects. The matrix is thresholded at ±2 to 6. Panel B displays the relationship between MMSE and age with brain connectivity by group. Confidence intervals are 95% BSRs. Panel C represents the positive BSR values from the covariance matrix (A) between MMSE, age, group, and functional connectivity in brain space. Panel D represents the negative BSR values. Panels A, C, and D are color coded by network: green represents the frontoparietal control network, red represents the dorsal attention network, and blue represents the default network. For panels C and D, within-network connections are colored according to network affiliation, and between-network connections are colored gray. See Fig. 1 caption for abbreviations.

cingulate, 2 posterior DN hub regions, were still fully integrated within the DN. The relative preservation of the DN along with greater between-network and hemispheric integration may support cognitive functioning in typical aging.

In contrast, this pattern of intrinsic functional connectivity appears to be insufficient to support cognitive functioning for individuals with MCI. Rather than these more circumscribed changes, cognitive performance in MCI was positively associated with a more

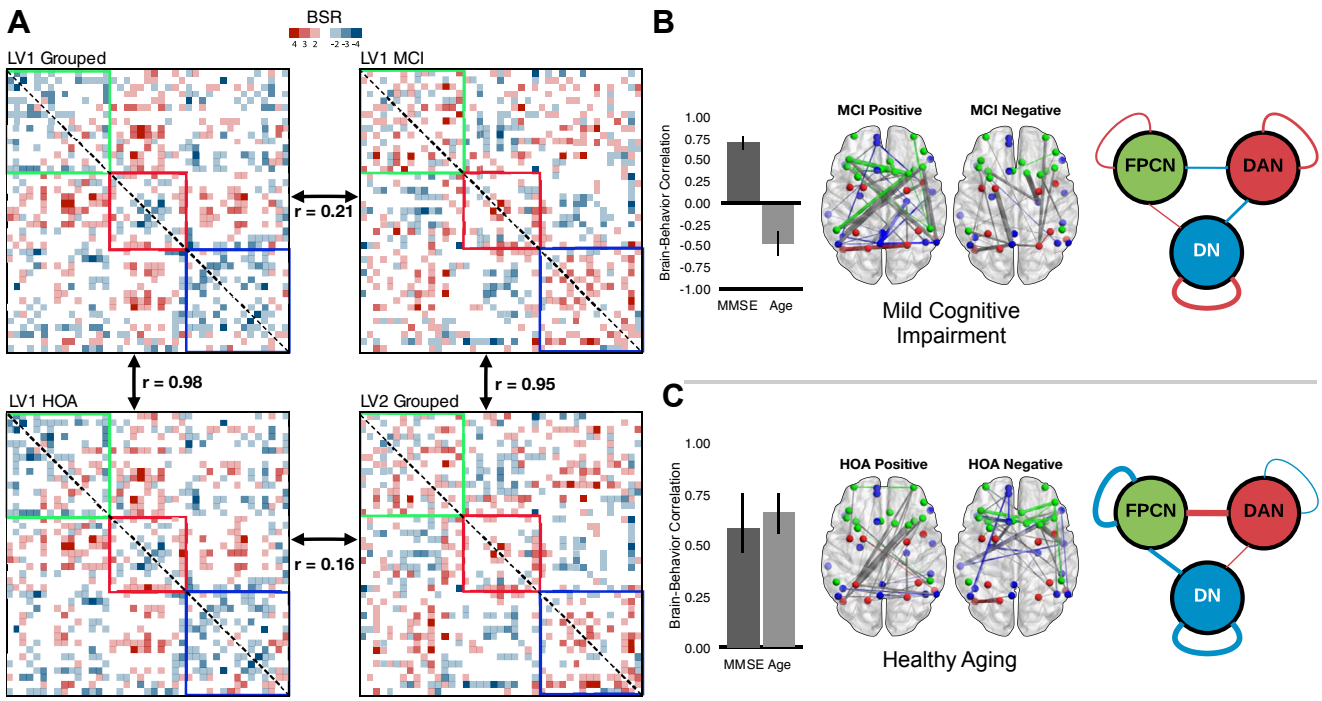

Fig. 4. Panel A shows the symmetrical BSR matrices from the between- versus within-group PLS analyses. Clockwise from top to left: the LV1 of the grouped analysis, the LV1 of the MCI group, the LV2 of the grouped analysis, and finally the LV1 of the HOA group. Each matrix is thresholded at ±2 to 6. Correlations between matrices were computed after vectorization. Panels B and C show the PLS results of the within-group analyses for MCI and HOA, respectively. Colors indicate network affiliation: green represents the FPCN, red represents the DAN, and blue represents the DN. For panels B and C, within-network connections are colored according to network affiliation, and between-network connections are colored gray. Error bars are 95% bootstrapped confidence intervals. Diagrams on the right-hand side of the figure represent the averaged BSR values within and between networks (blue represents negative BSR values, and red represents positive BSR values). Abbreviations: BSR, bootstrap ratio; DAN, dorsal attention network; DN, default network; FPCN, frontoparietal control network; HOA, healthy older adult; LV1, first significant latent variable; LV2, second significant latent variable; MCI, mild cognitive impairment; MMSE, Mini–Mental Status Examination; PLS, partial least squares.

generalized, spatially distributed pattern of intrinsic connectivity (see Fig. 2, panel D). This pattern encompassed nearly all of the ROIs included in our 3-network model and possibly reflects greater dedifferentiation and less specificity of brain function, a pattern that is commonly observed in older adulthood (Park et al., 2001). Whether this pattern reflects maladaptive compensatory processing in older adults continues to be an area of active debate (Grady, 2012; Spreng and Turner, in press). Our results suggest a more complex interaction. Although HOAs demonstrated a selective strengthening within a circumscribed set of cross-network connections to bolster performance, participants with MCI showed nonselective and more spatially distributed intrinsic functional connectivity changes that were associated with better cognitive functioning. We note, however, that this result for the participants with MCI from the between-group analysis should be interpreted cautiously due to the correlations from the within-group analyses that are described below.

The second network pattern associated with age and cognitive status identified a pattern of modular connections (greater within- and reduced between-network connectivity) that predict higher MMSE scores in HOAs regardless of age (see Fig. 3). As with the relationship between the first network pattern and the MCI group, this between-group analysis result for the HOAs also must be considered carefully in light of the results from the within-group analyses. The DN forms a distinct cluster with the precuneus as a centralized hub, as does the FPCN with the right middle frontal gyrus (BA 6). This positive association between a more young-like pattern of intrinsic functional connectivity and better cognitive performance in later life is consistent with previous research (Geerligs et al., 2015). In contrast, only younger individuals with MCI were able to maintain this more modular and compensatory-like organization. Modular functional brain organization declines with increasing age as within-module connections weaken, and regions become disconnected (Meunier et al., 2009), and normal aging has been shown to be associated with reductions in modularity and small worldness (Onoda and Yamaguchi, 2013). Consistent with our findings, further declines in local connectivity and modularity are observed with atypical aging and AD in relation to healthy controls (Brier et al., 2014; Supekar et al., 2008).

As a follow-up to our main analysis, we also examined each group separately. The first significant pattern of the between-group analysis, reflecting greater interactivity between brain networks and across hemispheres, correlated strongly with the within-group HOA results (Fig. 4). In contrast, the second significant pattern of the between-group analysis, reflecting changes within the DN, was more closely aligned to the within-group MCI results. This suggests that HOAs actively may recruit additional regions to support cognition, consistent with compensatory models such as the Posterior to Anterior Shift with Aging (PASA; Davis et al., 2008) and the Hemispheric Asymmetry Reduction in Older adults (HAROLD). In contrast, the pattern describing the MCI group suggests that to the extent these participants are able to preserve network integrity within the DN specifically, cognition is better preserved (e.g., Staffaroni et al., 2018).

To ensure that the functional connectivity network patterns derived were not specifically attributable to our selection of the MMSE as our cognitive measure (potentially biasing the findings as MMSE could have conceivably influenced determination of diagnostic status), we reproduced the main analyses using (1) immediate as well as (2) delayed memory scores and age. As shown in Supplementary Fig. 1, the primary between-group pattern of results from the main analysis was replicated for both immediate

memory and age, and for delayed memory and age. These additional analyses suggest that the effects we describe in the main analysis are stable and not driven our choice of the MMSE.

Previous functional connectivity studies of aging and dementia have focused primarily on changes within the DN (see Hafkemeijer et al., 2012; Damoiseaux, 2017 for a review). Our results suggest that the shifting interactivity of the DN with other large-scale brain networks in aging and brain disease may be equally important for understanding and mapping the functional network architecture of the brain to cognition in later life. The multivariate approach adopted here allowed us to investigate this possibility directly by modeling functional connections among all network nodes, as well as associations with cognition and age, across diagnostic groups within a single analytical model. In doing so, we identified functional connectivity differences between healthy aging older adults relative to those with MCI and determined that these differences vary by age and cognitive status. Specifically, the findings demonstrate that investigating changes in the DN in isolation cannot fully capture these differences. It is rather the dynamics of DN interactions with other large-scale brain systems that are necessary to fully elucidate the differences between healthy aging and MCI. Our results are consistent with the cascading model of functional network decline in AD (Jones et al., 2016). Early within-network changes of the DN precipitate later functional reorganization of large-scale systems, with declining compensatory gains as the disease progresses. Future work is necessary to better define the period in the disease course when these network changes transition from an indicator of resilience to a signal of more rapid cognitive decline.

Disclosure

The authors have no conflicts of interest to disclose.

Acknowledgements

This work was supported in part by a grant from the Alzheimer's Association (NIRG-14-320049) to RNS and CIHR grants to RNS and GRT. The authors thank Ryan Barker and Buddhika Bellana for their assistance. Data collection and sharing for this project were funded by the Alzheimer's Disease Neuroimaging Initiative (ADNI) (National Institutes of Health Grant U01 AG024904) and DOD ADNI (Department of Defense award number W81XWH-12-2-0012). ADNI is funded by the National Institute on Aging, the National Institute of Biomedical Imaging and Bioengineering, and through generous contributions from the following: AbbVie; Alzheimer's Association; Alzheimer's Drug Discovery Foundation; Araclon Biotech; BioClinica, Inc; Biogen; Bristol-Myers Squibb Company; CereSpir, Inc; Eisai Inc; Elan Pharmaceuticals, Inc; Eli Lilly and Company; EuroImmun; F. Hoffmann-La Roche Ltd and its affiliated company Genentech, Inc; Fujirebio; GE Healthcare; IXICO Ltd; Janssen Alzheimer Immunotherapy Research & Development, LLC.; Johnson & Johnson Pharmaceutical Research & Development LLC.; Lumosity; Lundbeck; Merck & Co, Inc; Meso Scale Diagnostics, LLC.; NeuroRx Research; Neurotrack Technologies; Novartis Pharmaceuticals Corporation; Pfizer Inc; Piramal Imaging; Servier; Takeda Pharmaceutical Company; and Transition Therapeutics. The Canadian Institutes of Health Research is providing funds to support ADNI clinical sites in Canada. Private sector contributions are facilitated by the Foundation for the National Institutes of Health (www.fnih.org). The grantee organization is the Northern California Institute for Research and Education, and the study is coordinated by the Alzheimer's Disease Cooperative Study at the University of California, San Diego. ADNI data are disseminated by the Laboratory for Neuro Imaging at the University of Southern California.

Appendix A. Supplementary data

Supplementary data associated with this article can be found, in the online version, at https://doi.org/10.1016/j.neurobiolaging.2018.10.001.

References

Andrews-Hanna, J.R., Smallwood, J., Spreng, R.N., 2014. The default network and self-generated thought: component processes, dynamic control, and clinical relevance. Ann. N. Y. Acad. Sci. 1316, 29–52.
Andrews-Hanna, J.R., Snyder, A.Z., Vincent, J.L., Lustig, C., Head, D., Raichle, M.E., Buckner, R.L., 2007. Disruption of large-scale brain systems in advanced aging. Neuron 56, 924–935.
Avelar-Pereira, B., Bäckman, L., Wåhlin, A., Nyberg, L., Salami, A., 2017. Age-related differences in dynamic interactions among default mode, frontoparietal control, and dorsal attention networks during resting-state and interference resolution. Front. Aging Neurosci. 9, 152.
Brier, M.R., Thomas, J.B., Fagan, A.M., Hassenstab, J., Holtzman, D.M., Benzinger, T.L., Morris, J.C., Ances, B.M., 2014. Functional connectivity and graph theory in preclinical Alzheimer's disease. Neurobiol. Aging 35, 757–768.
Brier, M.R., Thomas, J.B., Snyder, A.Z., Benzinger, T.L., Zhang, D., Raichle, M.E., Holtzman, D.M., Morris, J.C., Ances, B.M., 2012. Loss of intra- and inter-network resting state functional connections with Alzheimer's disease progression. J. Neurosci. 32, 8890–8899.
Buckner, R.L., 2004. Memory and executive function in aging and AD: multiple factors that cause decline and reserve factors that compensate. Neuron 44, 195–208.
Buckner, R.L., Andrews-Hanna, J.R., Schacter, D.L., 2008. The brain's default network: anatomy, function, and relevance to disease. Ann. N. Y. Acad. Sci. 1124, 1–38.
Buckner, R.L., Snyder, A., Shannon, B.J., LaRossa, G., Sachs, R., Fotenos, A.F., Sheline, Y.I., Klunk, W.E., Mathis, C.A., Morris, J.C., Mintun, M.A., 2005. Molecular, structural, and functional characterization of Alzheimer's disease: evidence for a relationship between default activity, amyloid, and memory. J. Neurosci. 25, 7709–7717.
Cabeza, R., 2002. Hemispheric asymmetry reduction in older adults: the HAROLD model. Psychol. Aging 17, 85–100.
Chan, M.Y., Park, D.C., Savalia, N.K., Petersen, S.E., Wig, G.S., 2014. Decreased segregation of brain systems across the healthy adult lifespan. Proc. Natl. Acad. Sci. U. S. A. 111, E4997–E5006.
Damoiseaux, J.S., 2017. Effects of aging on functional and structural brain connectivity. Neuroimage 160, 32–40.
Damoiseaux, J.S., Prater, K., Miller, B.L., Greicius, M.D., 2012. Functional connectivity tracks clinical deterioration in Alzheimer's disease. Neurobiol. Aging 33, 828.e19–828.e30.
Davis, S.W., Dennis, N.A., Daselaar, S.M., Fleck, M.S., Cabeza, R., 2008. Qué PASA? the posterior-anterior shift in aging. Cereb. Cortex. 18, 1201–1209.
Dennis, E.L., Thompson, P.M., 2014. Functional brain connectivity using fMRI in aging and Alzheimer's disease. Neuropsychol. Rev. 24, 49–62.
Folstein, M.F., Folstein, S.E., McHugh, P.R., 1975. "Mini-mental state". A practical method for grading the cognitive status of patients for the clinician. J. Psychiatr. Res. 12, 189–198.
Fox, M.D., Greicius, M., 2010. Clinical applications of resting state functional connectivity. Front. Syst. Neurosci. 4, 19.
Franzmeier, N., Buerger, K., Teipel, S., Stern, Y., Dichgans, M., Ewers, M., 2017. Cognitive reserve moderates the association between functional network anticorrelations and memory in MCI. Neurobiol. Aging 50, 152–162.
Geerligs, L., Renken, R.J., Saliasi, E., Maurits, N.M., Lorist, M.M., 2015. A brain-wide study of age-related changes in functional connectivity. Cereb. Cortex. 25, 1987–1999.
Grady, C.L., 2012. Trends in neurocognitive aging. Nat. Rev. Neurosci. 13, 491–505.
Grady, C.L., McIntosh, A.R., Horwitz, B., Rapoport, S.I., 2000. Age-related changes in the neural correlates of degraded and nondegraded face processing. Cogn. Neuropsychol. 17, 165–186.
Grady, C.L., Sarraf, S., Saverino, C., Campbell, K., 2016. Age differences in the functional interactions among the default, frontoparietal control, and dorsal attention networks. Neurobiol. Aging 41, 159–172.
Griffanti, L., Salimi-Khorshidi, G., Beckmann, C.F., Auerbach, E.J., Douaud, G., Sexton, C.E., Zsoldos, E., Ebmeier, K., Filippini, N., Mackay, C.E., Moeller, S., Xu, J.G., Yacoub, E., Baselli, G., Ugurbil, K., Miller, K.L., Smith, S.M., 2014. ICA-based artefact removal and accelerated fMRI acquisition for improved resting state network imaging. Neuroimage 95, 232–247.
Hafkemeijer, A., van der Grond, J., Rombouts, S.A., 2012. Imaging the default mode network in aging and dementia. Biochim. Biophys. Acta 1822, 431–441.
Jenkinson, M., Bannister, P., Brady, J.M., Smith, S.M., 2002. Improved optimisation for the robust and accurate linear registration and motion correction of brain images. Neuroimage 17, 825–841.
Jenkinson, M., Beckmann, C.F., Behrens, T.E., Woolrich, M.W., Smith, S.M., 2012. FSL. Neuroimage 62, 782–790.
Jenkinson, M., Smith, S.M., 2001. A global optimisation method for robust affine registration of brain images. Med. Image Anal. 5, 143–156.

Jones, D.T., Knopman, D.S., Gunter, J.L., Graff-Radford, J., Vemuri, P., Boeve, B.F., Petersen, R.C., Weiner, M.W., Jack, C.R., Alzheimer's Disease Neuroimaging Initiative., 2016. Cascading network failure across the Alzheimer's disease spectrum. Brain 139, 547–562.

Khan, U.A., Liu, L., Provenzano, F.A., Berman, D.E., Profaci, C.P., Sloan, R., Mayeux, R., Duff, K.E., Small, S.A., 2014. Molecular drivers and cortical spread of lateral entorhinal cortex dysfunction in preclinical Alzheimer's disease. Nat. Neurosci. 17, 304–311.

Krishnan, A., Williams, L.J., McIntosh, A.R., Abdi, H., 2011. Partial least squares (PLS) methods for neuroimaging: a tutorial and review. Neuroimage 56, 455–475.

Li, R., Wu, X., Fleisher, A.S., Reiman, E.M., Chen, K., Yao, L., 2012. Attention-related networks in Alzheimer's disease: a resting functional MRI study. Hum. Brain Mapp. 33, 1076–1088.

McIntosh, A.R., Bookstein, F.L., Haxby, J.V., Grady, C.L., 1996. Spatial pattern analysis of functional brain images using partial least squares. Neuroimage 3, 143–157.

McIntosh, A.R., Chau, W.K., Protzner, A.B., 2004. Spatiotemporal analysis of event-related fMRI data using partial least squares. Neuroimage 23, 764–775.

Meunier, D., Achard, S., Morcom, A., Bullmore, E., 2009. Age-related changes in modular organization of human brain functional networks. Neuroimage 44, 715–723.

Onoda, K., Yamaguchi, S., 2013. Small-worldness and modularity of the resting-state functional brain network decrease with aging. Neurosci. Lett. 556, 104–108.

Park, D.C., Polk, T.A., Mikels, J.A., Taylor, S.F., Marshuetz, C., 2001. Cerebral aging: integration of brain and behavioral models of cognitive function. Dialogues Clin. Neurosci. 3, 151–165.

Power, J.D., Barnes, K.A., Snyder, A.Z., Schlaggar, B.L., Petersen, S.E., 2012. Spurious but systematic correlations in functional connectivity MRI networks arise from subject motion. Neuroimage 59, 2142–2154.

Power, J.D., Barnes, K.A., Snyder, A.Z., Schlaggar, B.L., Petersen, S.E., 2013. Steps toward optimizing motion artifact removal in functional connectivity MRI; a reply to carp. Neuroimage 76, 439–441.

Salimi-Khorshidi, G., Douaud, G., Beckmann, C.F., Glasser, M.F., Griffanti, L., Smith, S.M., 2014. Automatic denoising of functional MRI data: combining independent component analysis and hierarchical fusion of classifiers. Neuroimage 90, 449–468.

Sanz-Arigita, E.J., Schoonheim, M.M., Damoiseaux, J.S., Rombouts, S.A., Maris, E., Barkhof, F., Scheltens, P., Stam, C.J., 2010. Loss of 'small-world' networks in Alzheimer's disease: graph analysis of FMRI resting-state functional connectivity. PLoS One 5, e13788.

Schultz, D.H., Cole, M.W., 2016. Higher intelligence is associated with less task-related brain network reconfiguration. J. Neurosci. 36, 8551–8561.

Seeley, W.W., Crawford, R.K., Zhou, J., Miller, B.L., Greicius, M.D., 2009. Neurodegenerative diseases target large-scale human brain networks. Neuron 62, 42–52.

Smith, S.M., 2002. Fast robust automated brain extraction. Hum. Brain Mapp. 17, 143–155.

Smith, S.M., Jenkinson, M., Woolrich, M.W., Beckmann, C.F., Behrens, T.E.J., Johansen-Berg, H., Bannister, P.R., De Luca, M., Drobnjak, I., Flitney, D.E., Niazy, R., Saunders, J., Vickers, J., Zhang, Y., De Stefano, N., Brady, J.M., Matthews, P.M., 2004. Advances in functional and structural MR image analysis and implementation as FSL. Neuroimage 23, 208–219.

Sorg, C., Riedl, V., Mühlau, M., Calhoun, V.D., Eichele, T., Läer, L., Drzezga, A., Förstl, H., Kurz, A., Zimmer, C., Wohlschläger, A.M., 2007. Selective changes of resting-state networks in individuals at risk for Alzheimer's disease. Proc. Natl. Acad. Sci. U. S. A. 104, 18760–18765.

Spreng, R.N., Sepulcre, J., Turner, G.R., Stevens, W.D., Schacter, D.L., 2013. Intrinsic architecture underlying the relations among the default, dorsal attention, and frontoparietal control networks of the human brain. J. Cogn. Neurosci. 25, 74–86.

Spreng, R.N., Stevens, W.D., Viviano, J.D., Schacter, D.L., 2016. Attenuated anticorrelation between the default and dorsal attention networks with aging: evidence from task and rest. Neurobiol. Aging 45, 149–160.

Spreng, R. N., & Turner, G. R. (forthcoming). Structure and function of the aging brain. In Samanez-Larkin, G. (Ed.), The Aging Brain. Washington, DC: American Psychological Association.

Spreng, R.N., Turner, G.R., 2013. Structural covariance of the default network in healthy and pathological aging. J. Neurosci. 33, 15226–15234.

Staffaroni, A.M., Brown, J.A., Casaletto, K.B., Elahi, F.M., Deng, J., Neuhaus, J., Cobigo, Y., Mumford, P.S., Walters, S., Saloner, R., Karydas, A., Coppola, G., Rosen, H.J., Miller, B.L., Seeley, W.W., Kramer, J.H., 2018. The longitudinal trajectory of default mode network connectivity in healthy older adults varies as a function of age and is associated with changes in episodic memory and processing speed. J. Neurosci. 38, 2809–2817.

Supekar, K., Menon, V., Rubin, D., Musen, M., Greicius, M.D., 2008. Network analysis of intrinsic functional brain connectivity in Alzheimer's disease. PLoS Comput. Biol. 4, e1000100.

Teipel, S., Grothe, M.J., Zhou, J., Sepulcre, J., Dyrba, M., Sorg, C., Babiloni, C., 2016. Measuring cortical connectivity in Alzheimer's disease as a brain neural network pathology: toward clinical applications. J. Int. Neuropsychol. Soc. 22, 138–163.

Tomasi, D., Volkow, N.D., 2012. Aging and functional brain networks. Mol. Psychiatry 17, 471–558.

Turner, G.R., Spreng, R.N., 2015. Prefrontal engagement and reduced default network suppression co-occur and are dynamically coupled in older adults: the default – executive coupling hypothesis of aging. J. Cogn. Neurosci. 27, 2462–2476.

Wang, K., Liang, M., Wang, L., Tian, L., Zhang, X., Li, K., Jiang, T., 2007. Altered functional connectivity in early Alzheimer's disease: a resting-state fMRI study. Hum. Brain Mapp. 28, 967–978.

Wang, P., Zhou, B., Yao, H., Zhan, Y., Zhang, Z., Cui, Y., Xu, K., Ma, J., Wang, L., An, N., Zhang, X., Jiang, T., 2015. Aberrant intra- and inter-network connectivity architectures in Alzheimer's disease and mild cognitive impairment. Sci. Rep. 5, 14824.

Wechsler, D., 1945. A standardized memory scale for clinical use. J. Psychol. 19, 87–95.

Whitfield-Gabrieli, S., Nieto-Castanon, A., 2012. CONN: a functional connectivity toolbox for correlated and anticorrelated brain networks. Brain Connect. 2, 125–141.

Xia, M., Wang, J., He, Y., 2013. BrainNet viewer: a network visualization tool for human brain connectomics. PLoS One 8, e68910.

Zhan, Y., Ma, J., Alexander-Bloch, A.F., Xu, K., Cui, Y., Feng, Q., Jiang, T., Liu, Y., Alzheimer's Disease Neuroimaging Initiative., 2016. Longitudinal study of impaired intra- and inter-network brain connectivity in subjects at high risk for Alzheimer's disease. J. Alzheimers Dis. 52, 913–927.